BUDKER INSTITUTE OF NUCLEAR PHYSICS

B.V. Chirikov and V.V. Vecheslavov

MULTIPLE SEPARATRIX CROSSING: CHAOS STRUCTURE

Budker INP 2000-1

NOVOSIBIRSK
2000

chaos structure

B.V. Chirikov and V.V. Vecheslavov

Budker Institute of Nuclear Physics
630090 Novosibirsk, Russia

Abstract

Numerical experiments on the structure of the chaotic component of motion under multiple crossing of the separatrix of a nonlinear resonance with time–varying amplitude are described with the main attention to the problem of ergodicity. The results clearly demonstrate nonergodicity of that motion due to the presence of a regular component of relatively small measure with a very complicated structure. A simple 2D–map per crossing has been constructed which qualitatively describes the main properties of both chaotic and regular components of the motion. An empirical relation for the correlation–affected diffusion rate has been found including a close vicinity of the chaos border where an evidence of the critical structure has been observed. Some unsolved problems and open questions are also discussed.

Email: chirikov@inp.nsk.su
Email: vecheslavov@inp.nsk.su

1 Introduction

The present work continues the studies of chaotic motion under a slow separatrix crossing. This is a particular case of adiabatic processes which are very important in physics because of the adiabatic invariance, approximate though, that is of the conservation of action variables (J) under a slow parametric perturbation. The main problem here is the degree of accuracy or of violation of that invariance. Separatrix crossing produces the largest chaotic component in phase space whose size does not depend on the adiabatic parameter $\epsilon \to 0$ which, however, does affect the detailed structure of the motion as well as its time scale.

In our previous paper [1] the single separatrix crossing for a particular model was described in detail. Remarkably, a fairly simple relation for such a model in Ref.[2] we used turned out to be surprisingly accurate within the most part of the chaotic component.

In this paper we discribe the results of numerical experiments on multiple separatrix crossing. We focus on statistical properties of the motion, including the structure and measure of regular component disseminated into the chaotic 'sea' in a rather tricky way. The existence of regular component means nonergodicity of the motion, the question which has remained unclear for a long time until recently. To our knowledge, the nonergodicity of motion in a similar model was first predicted theoretically and estimated numerically in Ref.[3]. We have confirmed this result by different methods, and found many other characteristics of the motion structure. The present work, as well as the previous one [1], was stimulated by a very interesting study of the corresponding quantum adiabaticity [4]. We use the same classical model which is briefly described, for reader's convenience, in the next Section (for details see Ref.[1]).

The model is specified by the Hamiltonian:

$$H(x,p,t) \;=\; \frac{p^2}{2} \;+\; A_0\,\sin(\Omega t)\cdot\cos x\,, \tag{2.1}$$

which describes a single nonlinear resonance in the pendulum approximation (see, e.g., Ref.[5, 6]) with a time–varying amplitude

$$A(t) \;=\; A_0\,\sin(\Omega t)\,. \tag{2.2}$$

The dimensionless adiabaticity parameter is defined in the usual way as the ratio of perturbation/oscillation frequencies:

$$\epsilon \;=\; \frac{\Omega}{\sqrt{A_0}}\,, \tag{2.3}$$

where $\sqrt{A_0}$ is constant frequency of the small pendulum oscillation for the maximal amplitude.

Two branches of the instant, or 'frozen', separatrix at some $t = const$ are given by the relation

$$p_s(x';t) \;=\; \pm 2\sqrt{|A(t)|}\cdot\sin\left(\frac{x'}{2}\right), \quad x' \;=\; \begin{cases} x, & A(t) > 0 \\ x-\pi, & A(t) < 0 \end{cases}\,. \tag{2.4}$$

Following previous studies of separatrix crossing we restrict ourselves below to this frozen approximation. As was shown in Ref.[1] the latter provides quite good accuracy of fairly simple theoretical relations.

In this approximation the action variable is defined in the standard way as

$$J \;=\; \frac{1}{2\pi}\oint p(x)\,dx\,, \tag{2.5}$$

where integral is taken over the whole period for x rotation (off the resonance) and over a half of that for x oscillation (inside the resonance). This difference is necessary to avoid the discontinuity of J at separatrix where the action is given by a simple expression

$$J \;=\; J_s(t) \;=\; \frac{4}{\pi}\sqrt{|A(t)|} \;\le\; J_{max} \;=\; \frac{4}{\pi}\sqrt{A_0}\,. \tag{2.6}$$

At $\Omega t \;=\; 0 \;\; (mod\,\pi)$ the action $J \;=\; |p|$, and the conjugated phase $\theta \;=\; x$. Notice that unlike p the action $J \ge 0$ is never negative.

transformation: $J/J_{max} \to J$. Then, the crossing region swept by separatrix is the unit interval, and J is simply related to the crossing time $t = t_{cr}$ by the expression

$$|A(t_{cr})| \;=\; J^2\,, \quad 0 \;\leq\; J \;\leq\; 1 \tag{2.7}$$

while the adiabaticity parameter becomes $\epsilon = \Omega$.

Numerical integration of the motion equations for Hamiltonian (2.1) was performed in $(x,\, p)$ variables using two algorithms. In most cases it was the so-called bilateral symplectic fourth-order Runge-Kutta algorithm as in Ref.[1]. However, in a few most long runs we applied a very simple and also symplectic first–order algorithm like in Ref.[2] which is actually the well known standard map [5] with the time–varying parameter:

$$\overline{\tilde{p}} \;=\; \tilde{p} \;+\; \tilde{A}_0 \cdot \sin\left(\tilde{\Omega}\tilde{t}\right) \cdot \sin x\,, \quad \overline{x} \;=\; x \;+\; \overline{\tilde{p}}\,, \tag{2.8}$$

where tilde marks the new set of quantities rescaled by the transformation

$$\tilde{A}_0 \;=\; \frac{1}{s^2}\,, \quad \tilde{t} \;=\; st\,, \quad \tilde{\Omega} \;=\; \frac{\Omega}{s}\,, \quad \tilde{p} \;=\; \frac{p}{s}\,. \tag{2.9}$$

Here s is the scaling parameter, and we remind that $A_0 = 1$. The primary goal of the rescaling was decreasing parameter $\tilde{A}_0$ which controls the computation accuracy. Usually, it was around $\tilde{A}_0 \approx 0.1$.

As is well known, the variation of J under adiabatic perturbation consists of the two qualitatively different parts: (i) the average action which is nearly constant between the crossings, up to an exponentially small correction, and which is of primary interest in our problem, and (ii) the rapid oscillation with the motion frequency. The ratio of the two time scales is $\sim \epsilon/\sqrt{|A(t)|} \ll 1$ which allows for efficient suppression of the second unimportant part of J variation by a simple averaging of $J(t)$ over a long time interval $\sim 1/\epsilon$ (see Ref.[1]).

3 Ergodicity

The ergodicity is the weakest statistical property in dynamical systems (see, e.g., Ref.[7]). Nevertheless, it is an important characteristic of the motion, necessary in the statistical theory (see, e.g., Ref.[8]).

The question of ergodicity of the motion under separatrix crossing remained open for a long time until recently. The upper bound for the measure (phase–space area) of a separate domain with regular motion ('stability islet') was estimated in Ref.[9] as $\mu_1 \lesssim \epsilon$.

first predicted theoretically and estimated numerically in Ref.[3]. The authors directly calculated the number and positions of stable trajectories for two different periods. Moreover, they were able to locate some of them in computation, and thus to measure their area in phase space which turned out to be surprisingly small.

Here, we make use of a different, statistical, approach. To this end, we first obtain from numerical experiments the steady–state distribution $f_s(J)$ in the action. In case of ergodic motion it should be constant. Examples of the distribution are shown in Fig.1 with the parameters listed in the Table below.

Table. Regular component under separatrix crossing

n	ϵ	$\mu_r \times 10^2$	$T \times N_{tr}$	N_b
1	0.1	0.68 ± 0.2	$2 \cdot 10^3 \times 1000$	200
2	0.05	0.75 ± 0.06	$4 \cdot 10^5 \times 200$	500
3	0.033	0.70 ± 0.2	$4 \cdot 10^5 \times 200$	200
4	0.033	0.81 ± 0.08	$4 \cdot 10^5 \times 150$	500
5	0.02	0.60 ± 0.05	$2 \cdot 10^6 \times 100$	200
6	0.01	0.75 ± 0.04	$4 \cdot 10^6 \times 100$	200

ϵ – parameter of adiabaticity
μ_r – total relative measure of regular component
T – number of separatrix crossings for each of N_{tr} trajectories
N_b – number of histogram bins in Fig.1
n – reference number for Fig.1

The striking feature of all the distributions is clear and rather specific inhomogeneity, reminiscent of a burst of 'icicles' hanging down from a nearly 'ergodic roof'. This directly demonstrates the generic nonergodic character of motion under separatrix crossing.

The histograms normalized in such a way that for ergodic motion the distribution $f_s(J) = 1$ while the sum over all the bins is also unity for any distribution. As a result the dips in the distribution ('icicles'), indicating the regular component, are compensated by an increase in the ergodic background. The latter is clearly seen in all distributions, especially for small J, and is a measure of the regular component. Namely, the relative measure (share) is given by the approximate relation

$$\mu_r \approx < f_s(J) - 1 >, \qquad J < J_1, \tag{3.1}$$

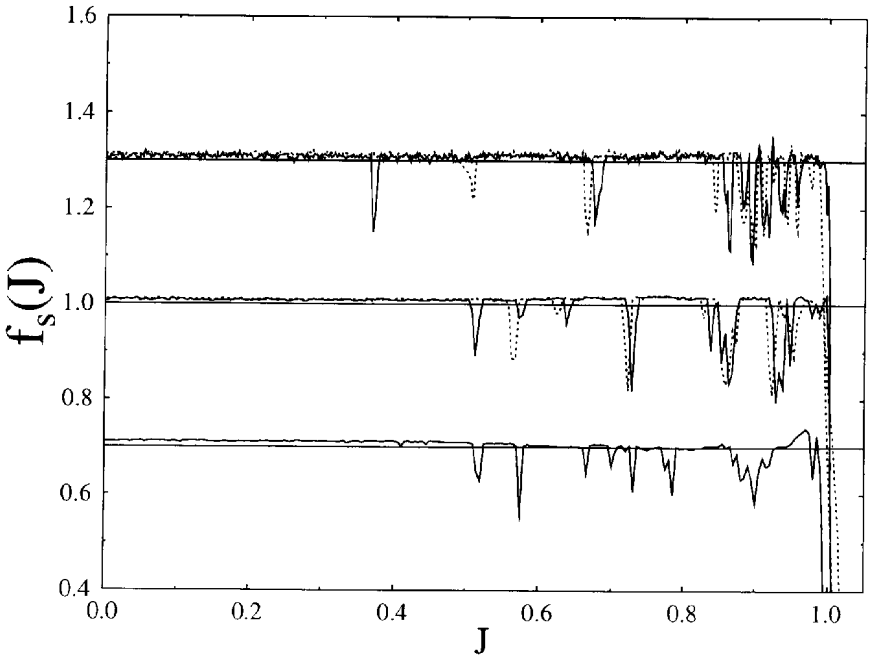

Figure 1: Histogram of the steady-state distribution for 3 values of ϵ (see Table): (n=4) upper curve shifted up by 0.3; (n=5) middle curve; and (n=6) lower curve shifted down by 0.3. Solid lines correspond to J values at $|A(t)| = 1$ while dotted ones are related to $A(t) = 0$ (see text).

where J_1 is the position of the first dip from below. The approximation comes from the border effects around $J = 1$ for any finite ϵ. Typically, at this theoretical border $f_s(1) \approx 0.5$, and drops to zero within the interval $|J-1| \sim \epsilon$. For this reason we used also other methods for measuring μ_r. One of them was the direct calculation of the area of dips in Fig.1. Scattering of the values provides an estimate for the accuracy of measurement of μ_r which is also given in the Table.

If we are interested in statistical data only, like in Fig.1, the computation of J value after each crossing is not necessary, nor is the averaging $J(t)$ done in Ref.[1]. This can be used for a further speed–up of the computation by applying simple relation $J = |p|$ at $A(t) = 0$ that is at each second passage between crossings (see Section 2 above). It is especially important for the

Fig.1. With the main standard code this also was used for calculating two different distributions, after odd and even passages. Both are shown in Fig.1 for cases n=4 and 5. The total regular area for the both is close, yet the positions of dips are different, sometime quite a lot. Another interesting peculiarity is the concentration of regular component near $J \approx 0.9$.

Even though the total regular area is very small ($\sim 1\%$) the local share of that can be as large as 20%. In spite of stability islets the chaotic component remains connected in the whole crossing region.

The dependence $\mu_r(\epsilon)$ is weak, if any. Apparently, the measured value is already close to the asymptotical one $\mu_r(0) \approx < \mu_r >= 0.0072$ where the average is taken over all six cases in the Table.

All this peculiarities will be further discussed in Section 5 below.

4 Diffusion, instability, and the critical structure

The diffusion in J was studied for a similar model in Ref.[2]. The essential difference from our model (2.1) was the restriction of separatrix oscillation (2.2): $A(t) > 0$ always. In this case the diffusive kinetics is valid in the whole crossing region. In our model the diffusive regime is restricted to the domain $J > \epsilon^{1/3}$ while for $J < \epsilon^{1/3}$ the ballistic regime takes over with a completely different kinetics (see Ref.[1] and below).

The diffusion rate in the random phase approximation (RPA) immediately follows from a simple expression for the change of J per separatrix crossing

$$\Delta J(J, \phi, \epsilon) = \mp \frac{\epsilon}{2} \cdot \frac{\sqrt{1 - J^4}}{J^2} \cdot \ln |2 \sin \phi| \,, \tag{4.1}$$

where the sign coincides with that of $\dot{A}(t)$, and is given by the relation:

$$D_0 = < (\Delta J)^2 >= \frac{\epsilon^2 \pi^2}{48} \left(\frac{1}{J^4} - 1 \right) \,, \tag{4.2}$$

where sub zero indicates RPA (see [2] and Ref.[14] therein).

Simple Eq.(4.1) was carefully checked in Ref.[1], and proved to be surprisingly accurate in the whole diffusive region $J > \epsilon^{1/3}$. However, as was shown already in Ref.[2] the correlation–free diffusion rate (4.2) holds true for a few crossings only (see also Ref.[1]). Afterwards, the correlation in ϕ builds up which decreases the diffusion rate D by a factor of 2. Here we

rate in comparison with the RPA theory (4.2). To this end we computed the correlation factor as the ratio

$$R(< J >) \;=\; \frac{< D >}{< D_0 >}\,. \tag{4.3}$$

It was done in the following way. A number of trajectories $N_{tr} = 100$ with initial $J = J_0$ and random x were run during $T = 800$ to 1600 separatrix crossings. Then, the empirical diffusion rate was calculated in the standard way:

$$< D >= \frac{< (J(T) - J_0)^2 >}{T}$$

with averaging over all the trajectories while the RPA theoretical rate $< D_0 >$ was computed by averaging expression (4.1) over all $N_{tr} \times T$ crossings. Altogether, 23 groups of trajectories with different initial J_0 in the whole range $0 \leq J_0 < 1$ (and random x) were run and related to the mean value $< J > \neq J_0$ over all the crossings. Actually, all $< J >$ values were found to lie off the ballistic domain because the trajectory quickly leaves the latter [1]. Nevertheless, for the initial $J_0 < \epsilon^{1/3}$ the trajectory spent some time within this domain, and we needed a certain empirical relation for the 'diffusion rate' there to perform averaging $< D_0 >$. That was obtained from the results in Ref.[1] in the form

$$D_0 \;=\; 0.16\,\epsilon^{2/3}, \qquad J \;<\; \epsilon^{1/3}.$$

It depends on ϵ but not on J.

The results of these numerical experiments are presented in Fig.2 in the log–log scale using the quantity $1 - < J >$ rather than $< J >$ as an argument. The reason for this is our special interest in the asymptotics $J \to 1$ at the chaos border in phase space on the edge of the crossing region. Typically, one would expect a very peculiar critical structure here (see, e.g., Ref.[8]). This interesting question will be discussed below in this Section.

So far, we show in Fig.2 the fit of the four leftmost points in the immediate vicinity of the chaos border to a power law expected in the critical structure. The result is:

$$R(J) \;=\; 1.05 \cdot (1 \;-\; J)^{0.25}\,. \tag{4.4}$$

Interestingly, this simple relation describes to a reasonable accuracy the rest of points as well except the five ones with smallest $< J >$ which are affected by the ballistic regime as explained below. Some clear deviations from smooth relation (4.4) reveal a certain fine structure of the diffusion of unknown origin.

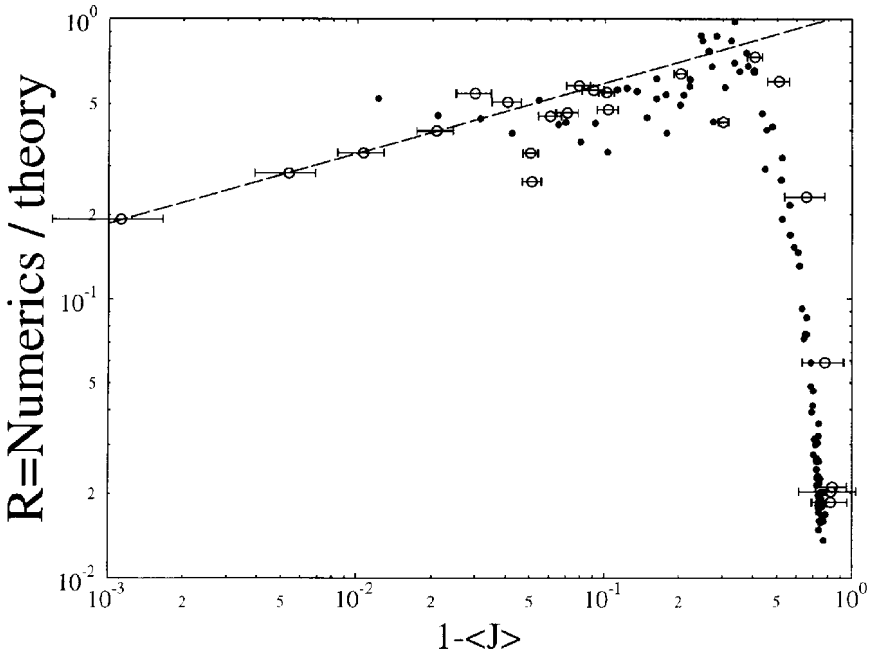

Figure 2: The ratio of empirical to theoretical diffusion rate (the correlation factor (4.3)) vs. the mean action $< J >$: $\epsilon = 0.001$ (circles); $\epsilon = 0.003$ (dots). Error bars show the spreading of trajectories during diffusion. The dashed straight line is fit (4.4) to four leftmost points ($\epsilon = 0.001$).

Factor $R < 1$ (4.3) is always less than one which means suppression of diffusion by the correlation. The minimal suppression (maximal R) occurs at $J = J_D \approx 5\epsilon^{1/3}$ which is much larger than the crossover to the ballistic region at $J = \epsilon^{1/3}$. This is the answer to the question about the width of the ballistic–affected region put forward in the conclusion of our previous publication [1]. For $J \lesssim J_D$ the correlation strongly suppresses diffusion down to a very low rate which is apparently determined by fluctuations. This unusual kinetics certainly deserves further studies. In any event, such a suppression explains a surprisingly long motion time required for a good steady–state distribution in Fig.1. The value of J_D marks the diffusion crossover from a big to small correlation (cf. Fig.3 below). In the complementary region $J \gtrsim J_D$ the correlation factor also decreases but very slowly only (4.4). Within fluctua-

see Section 5).

The diffusion rate itself is given by the following empirical relation:

$$D(J) \approx \frac{\pi^2}{48}\,\epsilon^2 \cdot \frac{(1-J^4)(1-J)^{1/4}}{J^4} \rightarrow \frac{\pi^2}{12}\,\epsilon^2 \cdot (1-J)^{c_D}\,, \qquad (4.5)$$

where the latter expression represents the asymptotics $J \to 1$, and $c_D \approx 5/4$ is the diffusion critical exponent.

A power law in Eq.(4.5) suggests the existence of a critical structure at the chaos border $J = 1$. Detailed study of this structure is hampered by some additional border effects as discussed above in Section 3. Even for fairly small $\epsilon = 0.001$ we managed to follow the asymptotic behavior to $1-J \sim 10^{-3}$ only (see Fig.2). Also, we are not able, as yet, to calculate the critical exponent c_D from the existing resonant theory of the critical phenomena [8]. However, there is another way to test this our conjecture. Namely, beside the local diffusion rate we might measure the asymptotics of the Lyapunov exponent $\Lambda(J)$. In fact, we did both simultaneously in the same run.

Positive Lyapunov exponent ($\Lambda > 0$) is the main condition for the strongest statistical properties in a dynamical system, including the randomness of most trajectories [10] (see also Ref.[11, 12]). The other condition for chaos is boundedness of the motion in the phase space. The first measurement of Λ, and in the same model, was reported in Ref.[13], just as a criterion for chaos. Formally, the Lyapunov exponent is defined in the ergodic theory of dynamical systems in the limit $t \to \infty$ [7] (as well as the diffusion rate, by the way). However, in case of rather different time scales of the motion the local Lyapunov exponent $\Lambda(J)$ becomes also meaningful and, moreover, a very important characteristic of the motion. Roughly, the ratio of time scales is that of error bars to corresponding J values in Fig.2 provided the number of crossings T per trajectory is sufficiently large for Λ to saturate.

In Fig.3 we present the results for $\Lambda(J)$ measured, as well as $D(J)$, per one separatrix crossing, and for the same parameters and initial conditions as in Fig.2. A clear crossover to asymptotic behavior is seen at $< J >= J_\Lambda \approx 0.8$. The latter was also fitted to a power law

$$\Lambda(J) \;=\; 0.98\,(1-J)^{c_\Lambda} \qquad (4.6)$$

with the critical exponent $c_\Lambda = 0.156$. In fitting we used ten leftmost points besides the two at $< J >= 0.95$ which represent some unknown fine structure (cf. Fig.2). Below crossover ($J < J_\Lambda$) the dependence is approximately linear:

$$\Lambda(J) \;\approx\; 1.9 \,-\, 1.4J\,. \qquad (4.7)$$

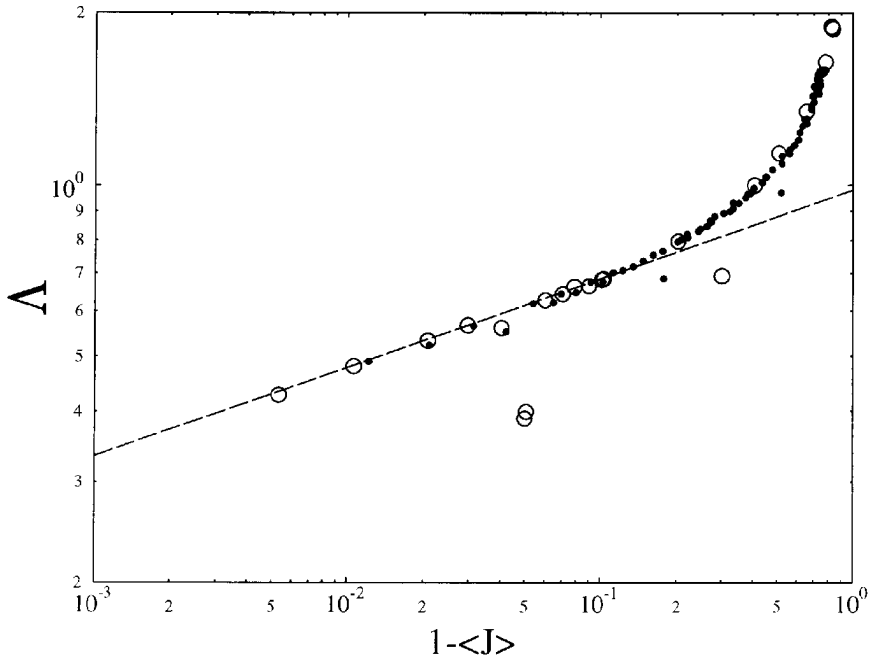

Figure 3: Lyapunov exponent Λ per crossing vs. mean action $< J >$: $\epsilon = 0.001$ (circles); $\epsilon = 0.003$ (dots). The dashed straight line is fit (4.6) to 10 leftmost points ($\epsilon = 0.001$).

The fluctuations are now much less than for $D(J)$. In both cases the dependence, if any, on ϵ is weak. Interestingly, no effect of the ballistic region is seen for $\Lambda(J)$ (cf. Fig.2).

Now, the theory of the critical phenomena [8] allows for calculation of ratio of the two exponents independent of other details of the critical structure. It is:

$$r_{th} = \frac{c_D}{c_\Lambda} = 8 \tag{4.8}$$

while the empirical value for this ratio from Eqs.(4.5) and (4.6) is $r_{exp} = 8.01$, a surprising agreement!

To illustrate this result more graphically we plot in Fig.4 the dependence

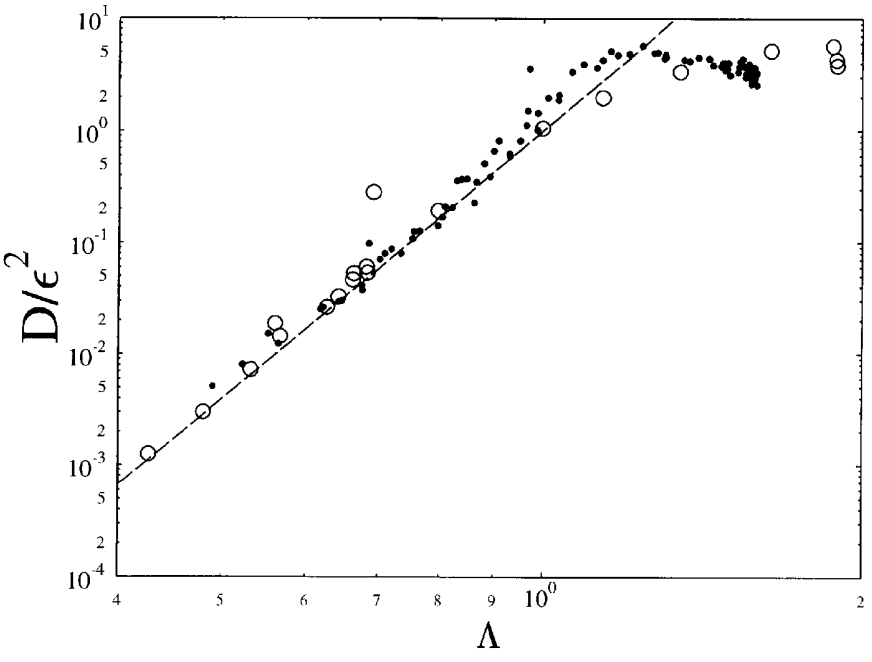

Figure 4: Diffusion rate vs. Lyapunov exponent: $\epsilon = 0.001$ (circles); $\epsilon = 0.003$ (dots). The dashed straight line is theoretical prediction for the critical structure (4.9).

$D(\Lambda)/\epsilon^2$ together with the expected asymptotic relation

$$\frac{D}{\epsilon^2} = \Lambda^8. \tag{4.9}$$

This appealing result strongly suggests the existence of a critical structure at the chaos border $J = 1$, and farther studies of this interesting problem are desired.

5 A simple map

Since the principal change in the adiabatic invariant J occurs at separatrix crossing it is natural to derive a 2D–map per crossing. This sort of maps were

cated, at least for a theoretical analysis. For the model under consideration here the global (in J) map has the form:

$$\begin{aligned} \overline{J} &= J \mp \tfrac{\epsilon}{2} \cdot \tfrac{\sqrt{1-J^4}}{J^2} \cdot \ln|2\sin\phi|\,, \\ \overline{\phi} &= \phi + \Phi(\overline{J})\,, \end{aligned} \tag{5.1}$$

where the sign coincides with that of $\dot{A}(t)$ (see Eq.(4.1)). The difficulty of constructing and using such a map lies in the second equation. Notice that both equations are approximate and cannot be a substitute for the exact motion equations even in the simplest form of another map (2.8).

For simplification the global map (5.1) we first transform it to a local one by the standard procedure, linearization of the second equation (see, e.g., Ref.[5, 6]):

$$\Phi(J) \to \pi n + \left(\frac{d\Phi}{dJ}\right)_{J=J_n} \Delta J\,. \tag{5.2}$$

Here the new parameter J_n satisfies the equation $\Phi(J_n) = \pi n$ with any integer n, and $\Delta J = J - J_n$. In our problem this approximation is fairly accurate for sufficiently small $\epsilon \to 0$. Particularly, we can consider discrete variable J_n as a continuous one (see below).

Typically, the derivative $\Phi' = d\Phi/dJ$ is still very complicated, and we assume another principal approximation. Namely, in calculating the change in ϕ between successive separatrix crossings we make use of the limiting motion frequencies neglecting the change of those near separatrix. They are:

$$\begin{aligned} \omega_r &= \tfrac{4}{\pi} \cdot J \qquad \text{for phase rotation}\,, \\ \omega_o &= \sqrt{A(t)} \quad \text{for phase oscillation}\,. \end{aligned} \tag{5.3}$$

The rotation frequency (off the resonance) remains constant between crossings while the oscillation one slowly varies due to separatrix motion. Now, the full period of phase ϕ, which is equal to π, corresponds to the full period of the rotation but only to half of that for the oscillation. Whence, the speed of ϕ variation in this approximation becomes:

$$\frac{d\phi}{dt} = \begin{cases} \frac{\omega_r}{2} = \frac{2}{\pi} J\,, & J > \sqrt{A(t)} \\ \omega_o = \sqrt{A(t)}\,, & J < \sqrt{A(t)}\,. \end{cases} \tag{5.4}$$

The latter inequalities determine transition from rotation to oscillation and back which occurs at the crossing time $t = t_{cr}$ where (see Eq.(2.7))

$$\epsilon t_{cr} = \arcsin(J^2)\,. \tag{5.5}$$

expressed in elementary functions as follows:

$$\Phi'(J) \;=\; \begin{cases} \frac{8}{\pi\epsilon}\left(\frac{1}{2}\arcsin\left(J^2\right) + \frac{J^2}{\sqrt{1-J^4}}\right), & J > \sqrt{A(t)} \\ -\frac{4}{\epsilon}\cdot\frac{J^2}{\sqrt{1-J^4}}, & J < \sqrt{A(t)}\,. \end{cases} \tag{5.6}$$

Since the most interesting part of motion structure is essentially concentrated near sufficiently large $J \approx 0.9$ (see Fig.1), we may leave in the first equation (5.6) the second term only with the factor $4/\epsilon$ from the second equation. In fact, the difference between the two factors is less than it appears just because of the contribution of the omitted term. However, the latter correction would be certainly an excess in accuracy for our rather crude map. Finally, we assume

$$\Phi'(J) \;\approx\; \pm\frac{4}{\epsilon}\cdot\frac{J^2}{\sqrt{1-J^4}}. \tag{5.7}$$

The local map is derived now from Eqs.(5.1), (5.2) and (5.7) in the standard way (see, e.g., Ref.[5, 6, 16]), and has the form:

$$\begin{aligned} \overline{P} \;&\approx\; P \mp K\cdot\ln\left|2\sin\phi\right| \bmod \pi\,, \\ \overline{\phi} \;&\approx\; \phi \mp \overline{P} + \tfrac{\pi}{4}\,, \end{aligned} \tag{5.8}$$

where the signs in both equations change simultaneously at each crossing, and where

$$P \;=\; \frac{4}{\epsilon}\cdot\frac{J_n^2}{\sqrt{1-J_n^4}}\cdot\Delta J \bmod \pi \tag{5.9}$$

is a new, local, momentum while the only parameter $K \approx 2$ is simply a constant in the approximation assumed. Additional phase change by $\pi/4$ comes from the shift of separatrix by π in x each time it crosses zero (see Eq.(2.4)). Literally, this change in ϕ is equal to $\pi/4 \pm \pi/4$ but the alternating part simply shifts P by a constant $\pi/4$ and, thus, can be omitted.

The phase space of the local map (5.8) is a 2D–torus $\pi \times \pi$. It approximately represents a narrow strip $\Delta_1 J \times \pi$ in the phase space of our main system (2.1) where

$$\Delta_1 J \;=\; \frac{\pi\epsilon}{4}\cdot\frac{\sqrt{1-J_n^4}}{J_n^2}. \tag{5.10}$$

For local map to be applicable the following two conditions are to be satisfied:

$$\frac{\Delta_1 J}{J_n} \;\approx\; \frac{\epsilon}{J_n^3} \lesssim 1 \tag{5.11}$$

$$\frac{\Delta_1 J}{1 - J_n} \approx \frac{\epsilon}{\sqrt{1 - J_n}} \lesssim 1 . \qquad (5.12)$$

The latter condition excludes a very narrow domain $1-J_n \lesssim \epsilon^2$, which is practically impossible to observe, while the former comprises the whole ballistic region.

The density of local strips (5.10) in J_n

$$\frac{dn}{dJ_n} \approx \frac{1}{\Delta_1 J} = \frac{4}{\pi\epsilon}\frac{J_n^2}{\sqrt{1 - J_n^4}} \qquad (5.13)$$

is rapidly increasing with J_n which explains the concentration of the regular component near the chaos border (Fig.1). This also explains the shift δJ of the dips between two different groups in Fig.1. The largest $\delta J \approx 0.15$ on the upper curve between the two leftmost dips is close to the full width of the corresponding local strip $\Delta_1 J \approx 0.16$.

An interesting feature of 4-step map (5.8) over a period of the adiabatic perturbation (four separatix crossings) is a singularity at $\phi = 0 \ (mod \ \pi)$. The Fourier spectrum of this singularity

$$\ln|2\sin\phi| = -\sum_{\mathrm{n=1}}^{\infty}\frac{\cos(2n\phi)}{n} \qquad (5.14)$$

is similar to that of the function with a finite discontinuity. As is well known (see, e.g., [17, 8] and references therein) the chaotic component of such a motion is always connected. It means that there is no invariant curve in the whole range $0 \le \phi \le \pi$ which would cut through and disconnect the chaotic component.

This confirms earlier conjectures on universality of chaos under separatrix crossings (see, e.g., Ref.[13]). Yet, the motion in such a system is typically nonergodic that is it contains a regular component. For a particular model under consideration it was first found in Ref.[3] and studied in detail in the present work (Section 3). Using simple map (5.8) we are able now to analyse and understand particular features of this less–known component of the motion.

To this end, we first measured the relative area μ_r of the regular component (stability islets) within the local phase–space cell $(\pi \times \pi)$ as a function of parameter K. The result is shown in Fig.5 (lower circles). In approximation of constant parameter K the relative area is the same in each cell, and hence is approximately equal to the relative area in the whole range of J in

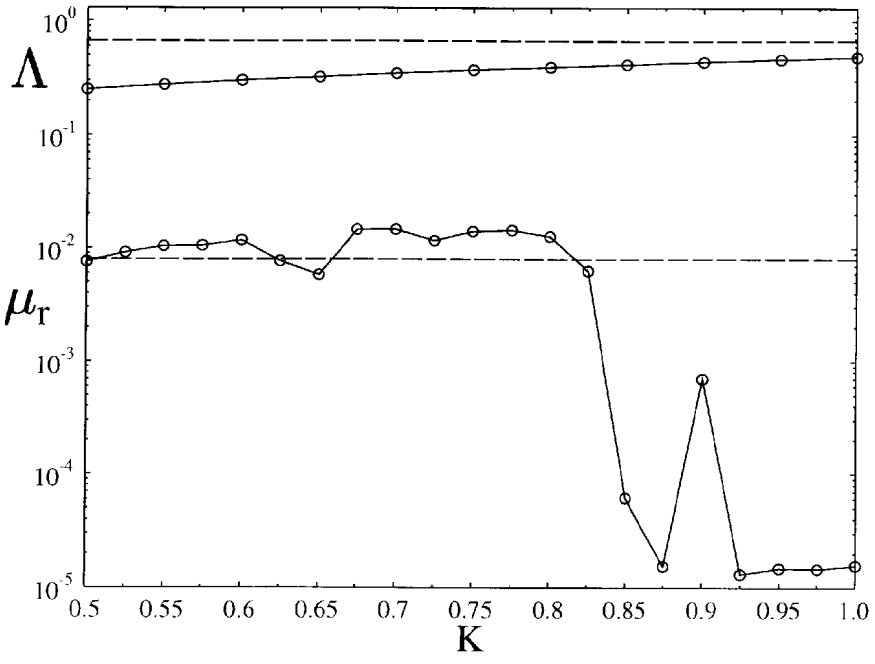

Figure 5: Comparison of local map (5.8) (circles connected by lines to guide the eye) and the main system (2.1) (dashed lines) with respect to: relative measure μ_r of regular component (lower data), and Lyapunov exponent Λ (upper data). For the main system the dashed lines give $\mu_r = 0.007$, and $\Lambda(J = 0.9) = 0.67$ (see text).

the main system. The latter is also shown in Fig.5 (lower dashed line). The agreement, within a factor of 2, seems reasonable provided local parameter $K \lesssim 0.8$ which is about half of the estimated value. Assuming $K \approx 0.8$ we may further compare the Lyapunov exponent in the local map (upper circles in Fig.5) with that of the main system at $J = 0.9$ the latter being larger by a factor of 2 (upper dashed line).

Thus, a simple local map (5.8) considered allows, beside a qualitative description, for even quantitative estimates within a factor of 2 which is not that bad for such a primitive map.

The local map does not depend on ϵ, and so do all the dimensionless quantities of the variables and the parameter of this map. Those include rel-

crossing (or per perturbation period)(Fig.3) as well as the correlation factor R (Fig.2) except small J close to the ballistic region where the local map is not applicable.

6 Conclusion

In the present work we studied the structure and statistical properties of the chaotic motion under separatrix crossing in numerical experiments with a typical model (2.1) used in such studies. An interesting distinction from previous studies (except Ref.[13]) is in that we allow the full swing of separatrix ($-1 \leq A(t) \leq 1$). In this case the chaos comprises the whole range ($0 \leq J \leq 1$), and there is only one chaos border at $J = 1$. Usually, the perturbation amplitude $A(t) > 0$ is strictly positive (or negative) which implies two chaos borders with the chaotic component between them ($0 < J_1 \leq J \leq 1$) but without an interesting ballistic region.

We have qualitatively confirmed previous results on the existence of regular component (nonergodicity) of the motion [3] as well as the correlation in chaotic component suppressing the diffusion [2], and found many other interesting details of the motion structure (Sections 3 and 4). For a physical interpretation and understanding of our empirical results we have constructed a very simple but meaningful local map per separatrix crossing which not only provides a qualitative description of the chaos structure but also allows for a reasonable quantitative estimates within a factor of 2.

In Fig.1 the most of regular component is seen near the chaos border, at $J \approx 0.9$. We never observed any at $J = 0$ at variance with the prediction in Ref.[14] based on the approximation of the motion equations by the Mathieu equation at small $\epsilon \to 0$. The resolution of this apparent contradiction is in that the amplitude of the parametric perturbation in the Mathieu equation increases $\sim \epsilon^{-2}$ (see Eq.(2.9)) so that the stable periodic solutions are only possible in special very narrow windows of ϵ. An interesting open question is the size of the corresponding stability islets.

Another interesting problem is the expected critical structure at the chaos border $J = 1$. The standard method - statistics of Poincare recurrences (see, e.g., [8] and references therein) - is difficcult to apply here because of the confusion with many internal chaos borders around stability islets of the regular component. Instead, we measured the asymptotics ($J \to 1$) of the two quantities, $\Lambda(J)$ and $R(J)$. Unfortunately, we were not able to calculate from the existing theory [8] the two critical exponents separately because of

of both (4.8) does not depend on the singularity and surprisingly well agrees with the empirical result (Fig.4). This is a strong evidence in favor of the critical structute which certainly deserves further studies.

In the present work, as well as in previous one [1] we studied the crossing of a single separatrix that is one of the two separatrix branches of a nonlinear resonance (see Eq.(2.4)). As is well known, there is another, related but not identical, process - the crossing of the whole resonance with both its branches. The latter was studied even much earlier [18] (see also Ref.[19]). From the beginning it was found that the change in adiabatic invariant per crossing: $\Delta J \sim \epsilon \ln \epsilon$ (in dimensionless variables) differs from that for separatrix crossing, calculated much later, by an additional factor $\ln \epsilon$ which slowly but indefinitely grows as $\epsilon \to 0$. The importance of this factor for the regular component of the motion was understood in Ref.[3]. Namely, it was theoretically predicted that the stable trajectories of the two particular periods are destroyed, together with the surrounding islets, for sufficiently small ϵ. An interesting open question is if the whole regular component, containing infinitely many islets [8], would vanish too, and how fast?

In terms of our local map (5.8) the additional factor would completely change all the structure of underlying motion because now the map parameter $K \sim |\ln \epsilon| \to \infty$ does depend on the adiabaticity parameter, and moreover indefinitely grows as $\epsilon \to 0$. It implies the dependence of all dimensionless characteristics of the motion on ϵ, in particular, the measure of regular component. We performed some preliminary numerical experiments to estimate the dependence $\mu_r(K)$. Asymptotically, it looks like an exponential which would imply a power law for $\mu_r(\epsilon)$.

In the very conclusion we would like to mention that the latter particular interestng question is a part of the general very important and very difficult unsolved problem in the theory of dynamical systems, the problem of ergodicity in case of analytic or even sufficiently smooth equations of motion.

Acknowledgements. This work was partially supported by the Russia Foundation for Fundamental Research, grant 97-01-00865.

[1] B.V. Chirikov and V.V. Vecheslavov, Adiabatic invariance and separatrix: Single separatrix crossing, preprint Budker INP 99–52, Novosibirsk, 1999; Zh. Eksp. Teor. Fiz. **117**, # 3 (2000).

[2] D. Bruhwiler and J. Cary, Physica D **40**, 265 (1989).

[3] A.I. Neishtadt, V.V. Sidorenko and D.V. Treschev, CHAOS **7**, 2 (1997).

[4] B. Mirbach and G. Casati, Phys. Rev. Lett. **83**, 1327 (1999).

[5] B.V. Chirikov, Phys. Reports **52**, 263 (1979).

[6] A. Lichtenberg and M. Lieberman, *Regular and Chaotic Dynamics*, Springer (1992).

[7] I. Kornfeld, S. Fomin and Ya. Sinai, *Ergodic Theory*, Springer, 1982.

[8] B.V. Chirikov, Chaos, Solitons and Fractals **1**, 79 (1991).

[9] Y. Elskens and F. Escande, Nonlinearity **4**, 615 (1991); Physica D **62**, 66 (1993).

[10] V.M. Alekseev and M.V. Yakobson, Phys. Reports **75**, 287 (1981).

[11] B.V. Chirikov, Open Systems & Information Dynamics **4**, 241 (1997).

[12] B.V. Chirikov and F. Vivaldi, Physica D **129**, 223 (1999).

[13] C. Menyuk, Phys. Rev. A **31**, 3282 (1985).

[14] F. Escande, in: *Plasma Theory and Nonlinear and Turbulent Processes in Physics*, Eds. V.G. Baryakhtar, V.M. Chernousenko, N.S. Erokhin, A.G. Sitenko and V.E. Zakharov, World Scientific, Singapore, 1988, p. 398.

[15] J. Cary and R. Skodje, Phys. Rev. Lett. **61**, 1795 (1988); Physica D **36**, 287 (1989).

[16] B.V. Chirikov, Particle dynamics in magnetic traps, in: *Voprosy teorii plasmy*,
13, Ed. B.B. Kadomtsev, Energoatomizdat, Moscow (1984), p. 3 (in Russian, English translation: *Reviews of Plasma Physics*, Vol. 13, Consultants Bureau, New York (1987), p. 1).

[17] I. Dana, N. Murray and I. Percival, Phys. Rev. Lett. **62**, 233 (1989).

[18] B.V. Chirikov, Dokl. Akad. Nauk SSSR **125**, 1015 (1959); B.V. Chirikov and D.L. Shepelyansky, Zh. Tekhn. Fiz. **52**, 238 (1982).

[19] J. Cary, F. Escande and J. Tennyson, Phys. Rev. A **34**, 4256 (1986).